Chapter 3

Methodology

A brief description of slope stability analysis and ant colony optimization is given in Chapter 1. However, comprehensive details of limit equilibrium analysis of slopes in the critical state, ACO characteristics and ACO algorithms to slope stability analysis are given in this chapter.

3.1 Limit Equlibrium Analysis for Slope Stability

As per the foregone discussion on Chapter 1, the slope stability assessment requires much analysis of different potential failure surfaces in order to obtain the minimum factor of safety. Generally, failure surfaces are neither linear nor circular. Therefore, many researchers have developed additional analysis methods to accommodate irregular shapes. The Bishop simplified method, Morgenstern-Price method, Spencer method are a few of them but most popular among the researchers. Each method uses different simplifying assumptions to overcome the problem of static indeterminacy, and thus produces slightly different results. Moreover, most limit equilibrium methods have four characteristics in common.

1) The factor of safety (F) is defined in relation to the shear forces acting upon the slip surface:

$$F = \frac{\tau_f}{\tau}, \tag{3.1}$$

where τ_f is the shear strength of soil and τ is the equilibrium shear stress along the shear surface.

2) Placing a factor on the shear strength is appropriate since evaluation of the shear strength typically involves the greatest uncertainty in practical applications of slope stability analyses. By the definition, the factor of safety is the same at all points along the potential slip surface. This is actually reasonable only at failure where the factor of safety is equal to unity.
3) The strength parameters are assumed independent of stress-strain behavior.
4) The equations equilibrium (some or all) are used to calculate the average values of τ and σ_n on each slice, where σ_n is the normal stress on the base of the slice. σ_n is required to determine the shear strength using the following equation:

$$\tau_f = c + \sigma_n \tan\phi\,, \tag{3.2}$$

where c and ϕ are Mohr-Coulomb strength parameters for cohesion and friction.

Figure 3.1 shows a typical potential sliding surface for a slope under a uniformly distributed overburden.

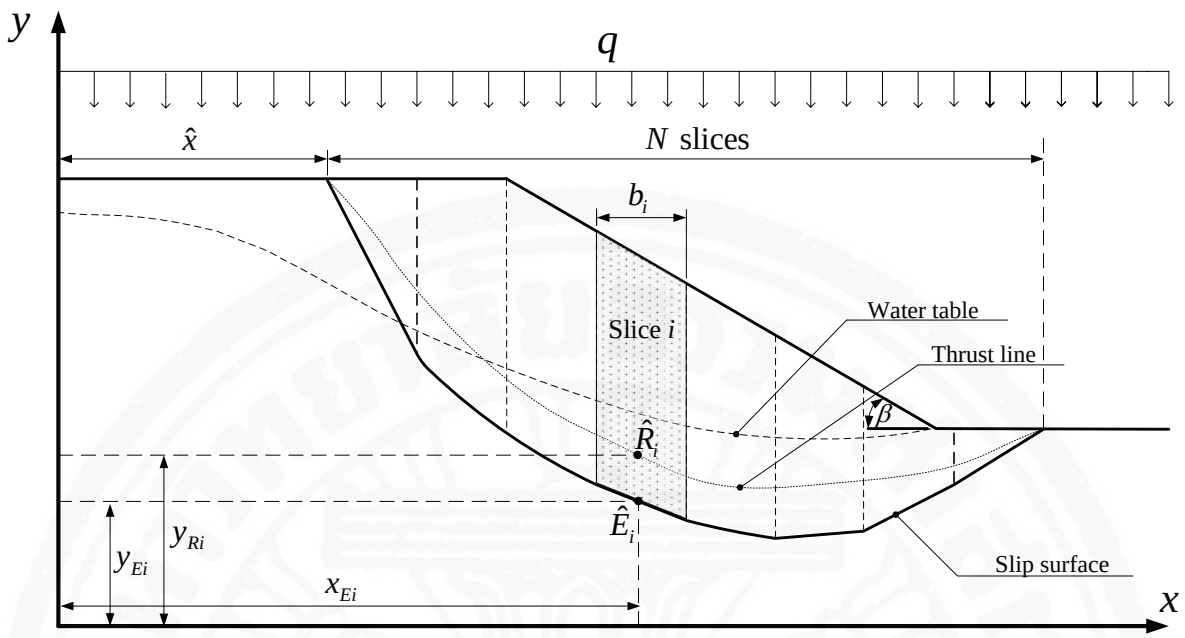

Figure 3.1 Typical potential sliding surface

For the purpose of analysis, the failing soil mass is divided into a finite number of vertical slices. The base of each slice represents the sliding surface. The portion of the sliding surface in each slice is assumed straight. Consequently, the sliding surface is represented as a piecewise-linear curve. Each slice is subjected to a system of internal and external forces when it is in equilibrium. Consider a typical i^{th} slice shown in Figure 3.2.

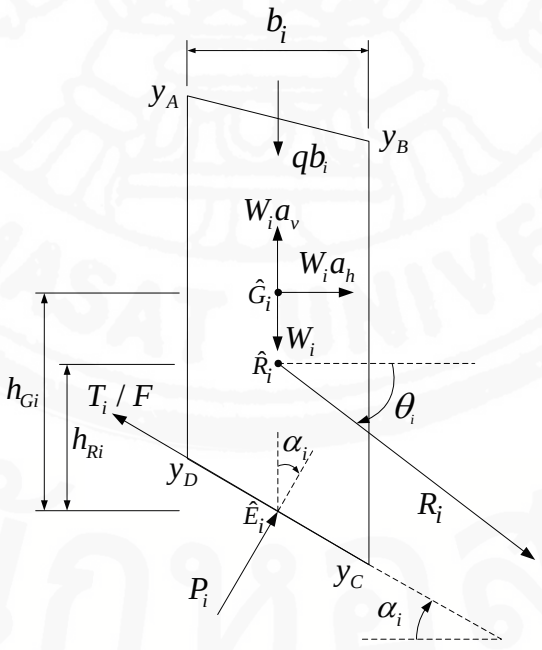

Figure 3.2 Inter-slice forces acting on i^{th} slice

In the Figure 3.2, y_A, y_B, y_C, and y_D denote the *y* coordinates of the four ends of the i^{th} slice. Further, point $\hat{G}_i$ presents the centre of gravity of the slice. At point $\hat{G}_i$, the weight of the slice W_i and the pseudo-static earthquake forces $W_i a_h$ and $W_i a_v$ are applied. Note that a_h and a_v, respectively, denote the pseudo-static coefficients for horizontal and vertical earthquake loading. On the two vertical boundary surfaces of the slice, there are in fact inter-slice forces. These forces are summed as the resultant inter-slice force R_i exerted at point $\hat{R}_i$. Also in the figure, qb_i represents the portion of the overburden force applied to the slice. On the sliding surface at the base of the slice, there are the resultant normal force P_i and the resultant shear force which is assumed to be equal to T_i / F, where T_i represents the shear resistance force of the soil and F represents the factor of safety. The location of inter-slice force is determined by using force and moment equilibrium as follows:

The weight of the i^{th} slice W_i is given by

$$W_i = \left\{ \frac{(y_A - y_D) + (y_B - y_C)}{2} \right\} b_i \gamma . \tag{3.3}$$

The total resultant normal force acting upon the base of the slice P_i can be expressed in terms of a force due to the effective stress P_i' and a force due to the pore water pressure u_i as

$$P_i = P_i' + u_i b \sec \alpha_i . \tag{3.4}$$

The mobilized shear force along the slip surface is given by the following equation, i.e.

$$T_{mi} = \frac{T_i}{F}. \tag{3.5}$$

From the Mohr-Coulomb failure criteria, we have

$$T_i = c' b_i \sec \alpha_i + P' \tan \phi', \tag{3.6}$$

$$T_{mi} = \frac{c' b_i \sec \alpha_i}{F} + \frac{P' \tan \phi'}{F}. \tag{3.7}$$

By considering the equilibrium in the direction normal to the slice base, we have

$$P_i + R_i \sin(\alpha_i - \theta_i) - W_i \cos \alpha_i + W_i a_v \cos \alpha_i + W_i a_h \sin \alpha_i - qb_i \cos \alpha_i = 0. \tag{3.8}$$

By considering the equilibrium in the direction parallel to the base of the slice, we have

$$\frac{T_i}{F} + R_i \cos(\alpha_i - \theta_i) - W_i \sin \alpha_i + W_i a_v \sin \alpha_i + W_i a_h \cos \alpha_i - qb_i \sin \alpha_i = 0 . \tag{3.9}$$

By substituting Equation (3.4) and Equation (3.7) in Equation (3.8) and Equation (3.9) and rearranging, we get

$$R_i = \frac{\frac{c'b_i \sec\alpha_i}{F} + \frac{\tan\phi'}{F}(W_i\cos\alpha_i - W_i a_v \cos\alpha_i - W_i a_h \sin\alpha_i - u_i b_i \sec\alpha_i + qb_i\cos\alpha_i) - W_i\sin\alpha_i + W_i a_h \cos\alpha_i - qb_i \sin\alpha_i}{\cos(\alpha_i - \theta_i)\left[1 + \tan(\alpha_i - \theta_i)\frac{\tan\phi'}{F}\right]}. \quad (3.10)$$

Here, ϕ' and C' denote the friction angle and the effective value of the coefficient of cohesion, respectively.

Taking the moment of all forces about the midpoint of slice base (point E_i) yields

$$h_{Ri} R_i \cos\theta_i + h_{Gi} W_i a_h = 0. \quad (3.11)$$

Subsequently, the y coordinate of point $\hat{R}_i$ in Figure 3.2 can be written as

$$y_{Ri} = y_{Ei} + h_{Ri} = y_{Ei} - (h_{Gi} W_i a_h / R_i \cos\theta_i). \quad (3.12)$$

The sum of overall moments of R_i's from all the slices about any arbitrary point must be zero. Selecting the origin as the point yields

$$\sum_{i=1}^{N} (y_{Ri} R_i \cos\theta_i + x_{Ei} R_i \sin\theta_i) = 0, \quad (3.13)$$

where N is the number of slices included in the failing mass. Substituting Equation (3.12) in Equation (3.13) gives

$$\sum_{i=1}^{N} (y_{Ei} R_i \cos\theta_i - h_{Gi} W_i a_h + x_{Ei} R_i \sin\theta_i) = 0. \quad (3.14)$$

Similarly, the sum of R_i's from all the slices must also be zero, i.e.

$$\sum_{i=1}^{N} R_i \cos\theta_i = 0, \quad (3.15)$$

$$\sum_{i=1}^{N} R_i \sin\theta_i = 0. \quad (3.16)$$

According to the Morgenstern-Price method (Morgenstern and Price, 1965), the ratio between the vertical and horizontal components of the inter-slice force is assumed to be in the form of $\lambda f(x)$. Here, λ is a constant. In addition, $f(x)$ is some appropriate function and x is the horizontal coordinate of the slice. For the i^{th} slice, this assumption is written as

$$\frac{R_i \cos\theta_i}{R_i \sin\theta_i} = \tan\theta_i = \lambda f(x_{Ei}). \quad (3.17)$$

In most cases, the function $f(x)$ is taken as one (Fredlund and Krahn, 1977; Spencer, 1967; Yamagami and Ueta, 1988; Zolfaghari et al., 2005) or $\sin cx$, where c is a constant (Fredlund and Krahn, 1977; Zhu et al., 2001). In this study, $f(x)$ is assumed to be one.

In this study, R_i in Equation (3.10) is substituted into Equations.(3.14) and (3.15) to give two nonlinear equations with two unknowns. The two unknowns are the factor of safety F and the constant λ. As aforementioned, the Newton-Raphson method is used in this study to solve the two equations for F and λ. The initial value of λ for the Newton-Raphson method is assumed to be an empirical value of $0.7\tan\beta$ (Zhu et al., 2001). Note that the angle β is the inclination of the slope surface defined in Figure 3.1. In addition, the initial value of F is assumed as one.

3.2 Concept of ACO

Ants are social insects. Their group behaviour leads to the survival of the whole colony. The most interesting behaviour of them is their foraging behaviour. When they work together, they have an ability to find the shortest path between their nest and a food source. This process is done by the use of a chemical substance called pheromone. Ants deposit pheromone on the ground while walking so that other ants can notice this pheromone trail and follow it to the food source. Moreover, when more paths are available from the nest to a food source, the ant colony can use pheromone trails left by individual ants to discover the shortest path to the food source and also back to the nest. It has been shown experimentally that these pheromone-trails laying and pheromone-trail following mechanisms play an important role for ants to discover the shortest path. The details of this real ant behaviour are explained in this section.

To demonstrate how an ant colony can find the shortest path, consider Figure 3.3. In the figure, there are two paths between the nest and a food source available with different distances. At the beginning, ants arrive to a decision point and the pheromone level is zero for each path. Therefore, all ants select both paths with equal probabilities and half of the ants tend to select each path. The ants choosing the short path are the first to reach the food source and to start their return to the nest which leads to a higher level of pheromone increase at the shorter path. Hence, this biases their decision for favouring the shorter path. Subsequently, due to the high level of pheromone in the shorter path, most ants will be attracted to the shorter path and ultimately all ants will select the shorter path to tour for their destinations. The dotted line in Figure 3.3 is approximately proportional to the amount of pheromone to the amount of pheromone deposed by ants. It is also noted that pheromone trails on each path is not permanent but rather they evaporated.

This simple foraging behaviour pattern results in development and design of heuristic algorithms for combinatorial optimization problems. The main underlying ideas emerge from the behaviour of real ants where a parallel search over several constructive computational threads based on local problem data and on a dynamic memory structure containing information on the quality of the previous solution. This ant based optimization principle combined with a pheromone update strategy, to avoid premature convergence to locally optimal solutions, can be applied to find a wide variety of combinatorial optimization problems.

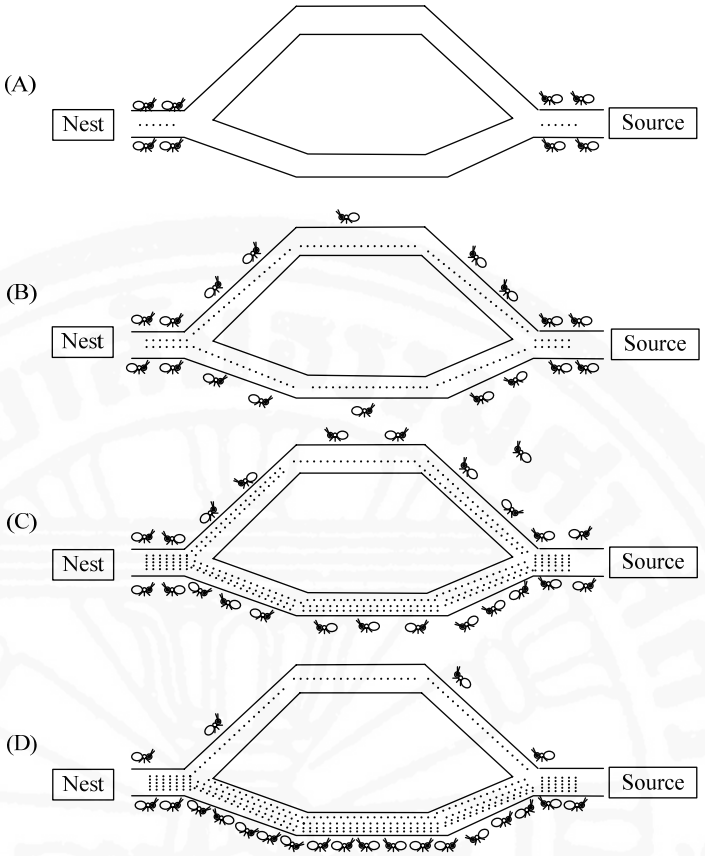

Figure 3.3 Real ant's behavior for finding shortest path:

(A) Ant reached at a decision point
(B) Both path are selected with equal probability and drop pheromone
(C) Pheromone level is higher on shorter path and more ants attract to it
(D) Finally all most ants select the shortest path by following higher level of pheromone

3.2.1 Characteristics of Artificial Ants

Artificial ants are simple computational agents that iteratively construct solutions for the instance. There are a few important characteristics possessed by real ants in order to formulate artificial ants and their ant algorithm.

1. An artificial ant algorithm consists of a finite number of ant populations. They work corporately like real ants. They are able to build feasible solutions while touring from problem states. The qualities of the solutions affect their decision making process for the next movement.

2. Artificial ants modify some of their characteristics according to the qualities of their partial solutions as natural ants do while their environment changes. The double bridge experiment (Dorigo et al., 1996) clearly shows changes of the selected path due to obstacles.
3. Real ants lay pheromone for their indirect communication to accomplish the task. Similarly, artificial ants lay pheromone referring to numerical information locally stored to create the artificial pheromone trails.
4. Real ants do not jump and they tour to the source by walking terrain to terrain. In the case of artificial ants, they also tour in subsequent steps through adjacent problem states.

3.2.2 Ant Path Searching Behavior

Each ant builds a solution to the problem by applying sequential decision policy starting from the source node. To move from the current node to the next node, an ant uses local information stored on the available sub-paths in a stochastic way to make its decision.

At the beginning of the search process, a constant amount of pheromone is dropped to the all available sub-paths. Ants move from node to node randomly without using any prior knowledge. Once they complete their tour to the destination node; ants are given limited form of memory in which they can store the partial paths they have visited so far as well as the quality of the links they have traversed. Through the use of memory, the ants can implement a number of useful behaviours that allow them to efficiently build solutions to the optimum solution of the problem as mentioned below.

1. Probabilistic solution making biased by pheromone trails, without forward pheromone updating.
2. Deterministic backward path with loop elimination and with pheromone updating.
3. Determination of the quantity of pheromone to be deposited based on the quality of the solutions generated.

3.2.3 Path Retracing and Pheromone Updating

When reaching the destination node, the ant switches from the forward mode to the backward mode and then retraces step by step the same path backwards to the source node. During its return tour to the nest, the ant deposits pheromone whose amount is proportional to the quality of the path. This subsequently increases the amounts of pheromone on all the sub-paths that comprise the whole path.

3.2.4 Pheromone Trail Evaporation

The process of pheromone trail evaporation is done as an exploration mechanism that prevents quick convergence of the entire ants towards a suboptimal path. In fact, the reduction in pheromone concentration favours the exploration of various paths during the entire search process. In real ant colonies, pheromone also evaporated, but in the case of artificial ants, this phenomena is utmost important probably due to the fact that the

optimization problems tackled by artificial ants are much more complicated than those real ants can solve. A mechanism like evaporation allows a continuous improvement of the "learned" problem structure and enables them to reach the optimum solution.

3.3 An Ant Colony Optimization for Finding the Critical Failure Surface in Slopes

The concept and methodology employed by the Ant Colony Optimization heuristic method used in this study is more similar to the routine used by Nanakorn et al. (2002) for sizing optimization of steel structures. In their study, ants were used to find possible structures. By minimizing an objective function and an error term, ants were able to find the optimum structure with the minimum weight. In this study, ants are used to find the optimum slip surface instead of the optimum truss structure. In addition, the factor of safety pertaining to the selected surface is solved by two nonlinear equations formulated by the Morgenstern-Price method.

3.3.1 Representation of Slip Surfaces

Before starting the ACO search, the slope has to be defined with its governing geotechnical parameters. In this study, the slope is always defined from the upstream on the left side to the downstream on the right side. Hence, the failure mass always moves from left to right. The total search area is selected with adequate ranges for failure initiation and termination. This is problem specific and the ranges are selected by careful observation of possible search patterns in order that every possible failure for a given slope is accommodated. Initially, the slope is divided into a finite number of slices with a predefined slice width. The failing soil mass is subdivided into N slices. Subsequently, a slip surface is represented as a piecewise-linear curve with N intervals as shown in Figure 3.1. In the figure, $\hat{x}$ denotes the horizontal coordinate of the initiation point of the slope failure. In addition, α_i represents the angle of the slip surface for the i^{th} slice measured in the clockwise direction from the horizontal axis as defined in the Figure 3.2. Furthermore, the angular changes between two successive failure lines $\Delta\alpha_i$ are defined for representing the rest of the failure surface. It should be noted that, except for α_1, α_i's are not directly used in the representation of slip surfaces and $\Delta\alpha_i$'s are used instead. This is because, if α_i's are directly used, it will be difficult to prevent obviously unrealistic slip surfaces such as zigzag curves from being included in the search space. Moreover, $\Delta\alpha_i$ is defined as $\Delta\alpha_i = \alpha_{i+1} - \alpha_i$. This allows the tours of unrealistic failure surfaces to be omitted easily and makes each failure surface kinematically admissible. Figure 3.4 illustrates the concept of using $\Delta\alpha_i$ rather than using angle α_i, which enables the criteria of $\alpha_1 > \alpha_2 > \cdots > \alpha_{n-1} > \alpha_n$ for admissible failure surfaces. From the problem configuration used in this study, the soil mass is always assumed to slide to the right. As a result, $\Delta\alpha_i$ is always assumed negative in order to avoid unrealistic slip surfaces.

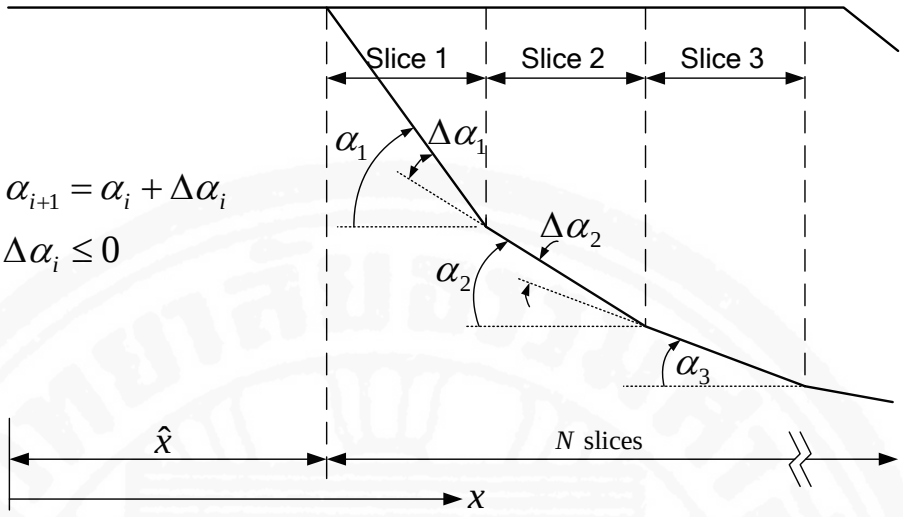

Figure 3.4 Representation of an admissible failure surface

Once the governing parameters are defined, the variable vector for finding an optimum failure slope by ACO can be declared thereby. Since the failure mass is divided into N number of slices, hence there are N+1 of variables associated with the problem. Define the variable vector $\mathbf{A}$ to represent slip surfaces in the ACO process as

$$\mathbf{A} = \begin{bmatrix} A_1 & A_2 & \cdots & A_{N+1} \end{bmatrix}^T = \begin{bmatrix} \hat{x} & \alpha_1 & \Delta\alpha_1 & \Delta\alpha_2 & \cdots & \Delta\alpha_{N-1} \end{bmatrix}^T. \tag{3.18}$$

Figure 3.5 shows how each vector $\mathbf{A}$ is interpreted as a slip surface. In general, from the initiation point, the slip surface follows exactly the piecewise-linear curve represented by $\mathbf{A}$. Nevertheless, once the piecewise-linear curve intersects the soil boundary, the slip surface follows the soil boundary instead. If the piecewise-linear curve does not intersect the soil boundary at all, the curve is considered infeasible. In addition, if the vertical distance from the intersecting point to the top of the slope is less than half of the slope height, the curve is interpreted as a local failure and, as a result, it is considered infeasible.

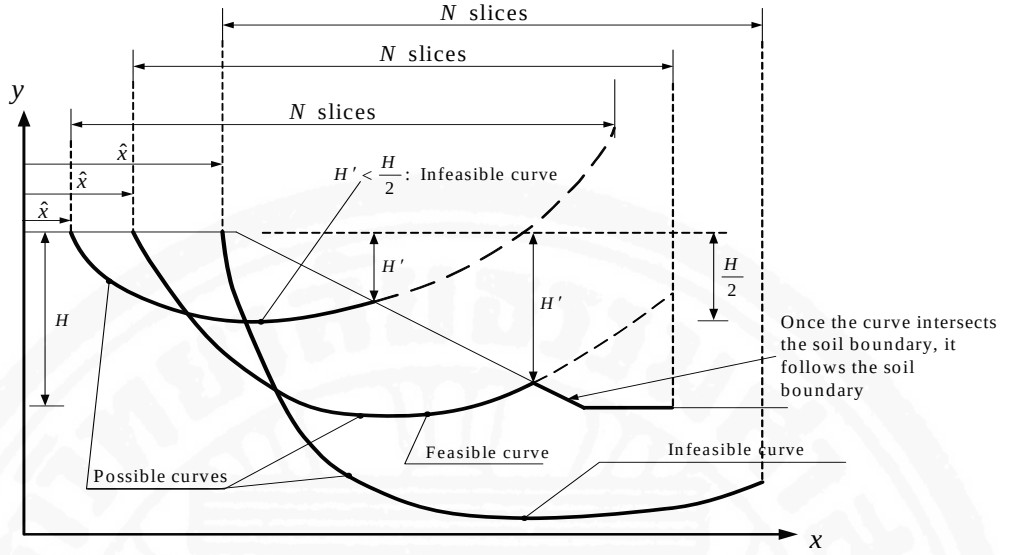

Figure 3.5 Feasible and infeasible curves

The search range for the horizontal coordinate of the initiation point of the slope failure $\hat{x}$ is selected by carefully observing the problem itself. The precision of the values of $\hat{x}$ is equal to the slice width. Therefore, the smaller slice width gives the smaller snapping distance for the failure initiation point. In this study, α_1, which represents the starting angle of the slip surface, is selected around the Rankine failure angle range, i.e. in between $45^\circ - \frac{\phi}{2}$ to $45^\circ + \frac{\phi}{2}$. Here, ϕ represents the coefficient of cohesion of the failure initiation soil layer. For an example, if the value of $\phi = 30^\circ$, then the range will be in between $30°$ and $60°$ for the angle α_1. The precision can be set according to the complexity of the problem and more precision enables more explorations of possible slip surfaces. The range of $\Delta\alpha_i$ is selected through a reasonable range by carefully observing an informed possible search patterns.

3.3.2 ACO Algorithm

The concept of the foregone discussion can be now transformed to the ACO algorithm for finding the critical failure surface of a given slope. To find the critical failure surface, the combination of the variables in $\mathbf{A}$ that yields the minimum factor of safety has to be found. Define the quality function $Q(\mathbf{A})$ for measuring the quality of slip surfaces as

$$Q(\mathbf{A}) = \frac{1}{1 + F(\mathbf{A})}. \tag{3.19}$$

Here, $F(\mathbf{A})$ is the factor of safety for the slip surface represented by $\mathbf{A}$. It can be seen that slip surfaces that have smaller factors of safety will result in larger values of $Q(\mathbf{A})$. Finding the slip surface that yields the minimum factor of safety can now be expressed as a

maximization problem of $Q(\mathbf{A})$. In this study, a very large value of the factor of safety F is used for every infeasible curve.

To maximize the quality function $Q(\mathbf{A})$ with respect to slip surfaces, the proposed ACO algorithm is structured as shown in Figure 3.6.According to the algorithm, artificial ants will make artificial tours from the starting node on the left to the end node on the right. During each tour, each artificial ant will select $\hat{x}$, α_1 as well as $\Delta\alpha_1$ to $\Delta\alpha_{N-1}$ from the available lists of values. For each variable, the available values are the available sub-paths one of which the ant must select to traverse. The combination of the variables obtained from the selection becomes the path that the ant has walked and will be interpreted as a slip surface. In Figure 3.6, A_i^1 to $A_i^{S_i}$ denote the available values or the available sub-paths for variable A_i. Here, S_i denotes the number of the available sub-paths for variable A_i.

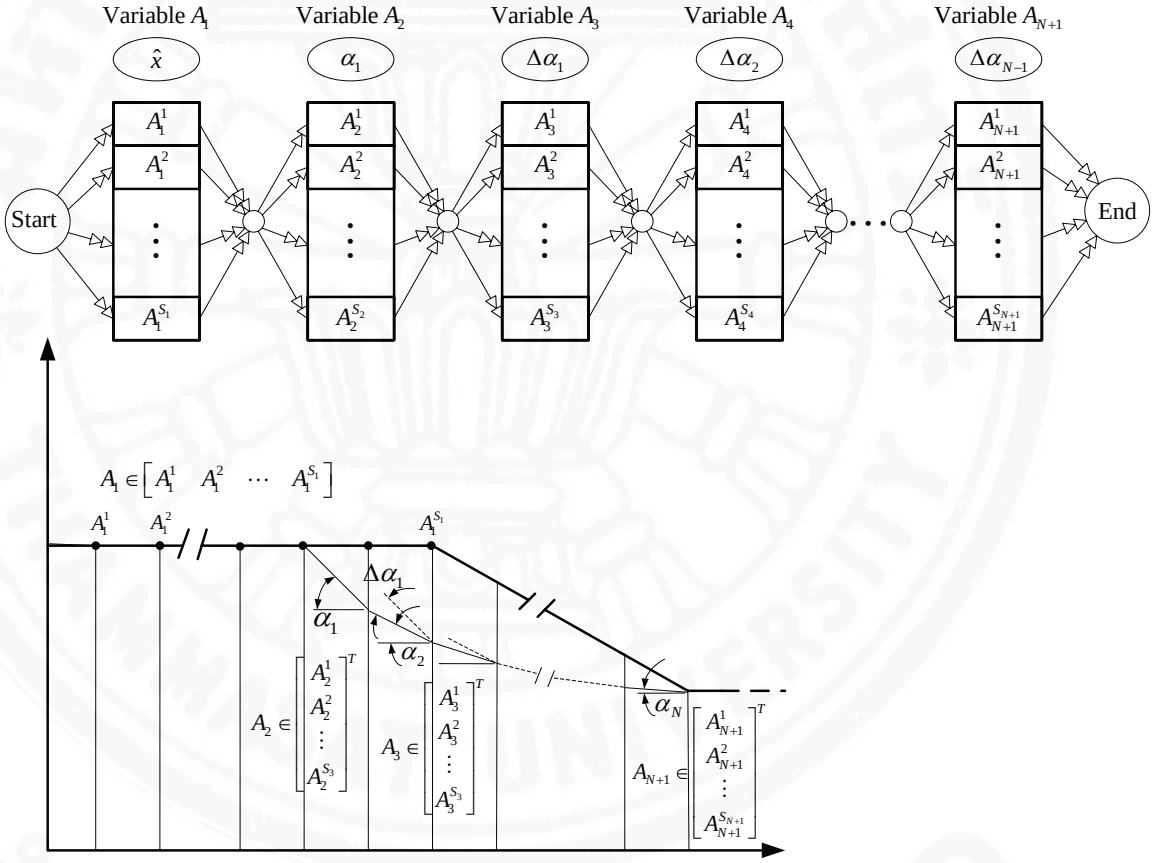

Figure 3.6 Example of slope stability analysis by the ACO approach

For the ACO to work, artificial ants will have to make many artificial tours and they must obey the following simple rules:

1) Ants will probabilistically select paths with higher levels of pheromone. In other words, paths with higher pheromone levels will have higher chance to be selected by ants.

2) The amount of pheromone laid by an ant on the path, which it has walked, depends upon the quality of the path. If the path is of high quality, the ant that has walked the path will lay a large amount of pheromone on the path. For slope stability analysis, a path is considered high quality if it represents a slip surface with a low factor of safety.

These two rules, though simple, are enough for the colony to perform its task. The first rule can be implemented by setting the probability of a sub-path being selected by an ant in tour *t* as

$$p(A_i^a,t)=\frac{\tau(A_i^a,t)}{\sum_{k=1}^{S_i}\tau(A_i^k,t)}. \tag{3.20}$$

Here, $p(A_i^a,t)$ denotes the aforementioned probability where A_i^a represents the a^{th} sub-path for variable A_i. In addition, $\tau(A_i^a,t)$ denotes the amount of pheromone of sub-path A_i^a in tour *t*.

To implement the second rule of ants, the quality function $Q(\mathbf{A})$ defined in Equation 3.21 is used for the quality evaluation of paths. The amount of pheromone to be laid on a path can be directly set to be proportional to the value of $Q(\mathbf{A})$ for the path. However, the difference between the quality values given by $Q(\mathbf{A})$ of the best and average paths varies tour by tour. In early tours, the difference can be very large and the best paths become relatively too good. As a result, premature convergence may be obtained. In later tours, the difference can be very small and the average paths become almost as good as the best paths. As a result, the search may become a random walk. To prevent all of these problems, the quality function is usually scaled into a specified positive range. Many scaling schemes have been proposed for heuristic optimization methods (Goldberg, 1989; Grefenstette, 1986; Michalewicz, 1996; Nanakorn et al., 2002). In this study, a bilinear scaling technique shown in Figure 3.8 will be used. In the figure, the subscripts min, max, and avg denote the minimum, maximum and average values, respectively. In addition, Z is a user-defined constant. The scaled quality function Q^{sc} will be used in the subsequence calculation instead of Q.

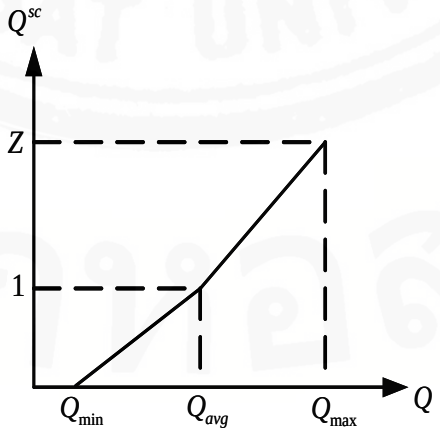

Figure 3.7 Bilinear scaling for the quality function

By employing the general procedure for ACO algorithms (see, for example, Gutjahr (2000)), the pheromone-trail-laying algorithm can be constructed. To this end, denote the vector **A** selected by ant Ant_j during tour *t* as $\mathbf{A}(Ant_j, t)$ and define a function $\Delta\tau$ as

$$\Delta\tau(A_i^a, Ant_j, t) = \begin{cases} Q^{sc}[\mathbf{A}(Ant_j, t)]/(N+1) & : \text{if } Ant_j \text{ has traversed } A_i^a \text{ during tour } t, \\ 0 & : \text{otherwise.} \end{cases} \quad (3.21)$$

Note that $N+1$ is the number of the variables in **A**. Define a function V as

$$V(t) = \sum_{j=1}^{M} Q^{sc}[\mathbf{A}(Ant_j, t)], \quad (3.22)$$

where *M* denotes the number of the ants. It can be seen that *V*(*t*) is actually the summation of the value of $\Delta\tau$ in tour *t*.

Next, define a function $\Delta\bar{\tau}$ as

$$\Delta\bar{\tau}(A_i^a, t) = \frac{\sum_{j=1}^{M} \Delta\tau(A_i^a, Ant_j, t)}{V(t)} \quad (3.23)$$

Finally, define the pheromone-updating scheme as

$$\begin{aligned} \tau(A_i^k, t) &= 1 \Big/ \sum_{i=1}^{N+1} S_i && t = 1, \\ \tau(A_i^k, t+1) &= (1-\rho_1)\tau(A_i^k, t) + \rho_1 \Delta\bar{\tau}(A_i^k, t) && t = 1, \\ \tau(A_i^k, t+1) &= (1-\rho)\tau(A_i^k, t) + \rho \Delta\bar{\tau}(A_i^k, t) && t \geq 2, \end{aligned} \quad (3.24)$$

where ρ denotes the evaporation factor. This factor is used to control the evaporation rate. In addition, ρ_1 denotes the evaporation factor used only for the first tour. It can be seen from Equation 3.24 that, at the beginning of the first tour, all sub-paths receive the same initial amounts of pheromone and the sum of these initial amounts of pheromone from all sub-paths is equal to one. In the first tour, since the amounts of pheromone on all sub-paths are the same, the ants select their paths basically at random. After that, the evaporation is implemented by the term $(1-\rho_1)\tau(A_i^k, t)$ while the pheromone laying is implemented by the term $\rho_1 \Delta\bar{\tau}(A_i^k, t)$. The initial pheromone is introduced at the beginning of the first tour in order to make certain that there is no sub-path that has a zero amount of pheromone at the end of the first tour. Any sub-path that has a zero amount of pheromone will never have any chance to be selected by any ants and will subsequently never obtain any pheromone. As a result, it is as if they are removed from the problem. Since the initial pheromone is used just to prevent sub-paths from having no pheromone, a large evaporation rate ρ_1 is used in the first tour to reduce its effect in the subsequent tours. From the second tour, the evaporation is implemented by the term $(1-\rho)\tau(A_i^k, t)$ and the pheromone laying is implemented by the term $\rho \Delta\bar{\tau}(A_i^k, t)$. It can be seen from Equations (3.23)-(3.26) that, at the end of every tour,

the sum of pheromone values of all sub-paths always remains equal to one. The complete algorithm can be summarized as

Tour=1;

Lay the initial pheromone on all sub-paths;

All ants select paths randomly;

Calculate paths' quality;

Find the best solution of the tour;

Update the best solution of all tours;

With a large evaporation rate, existing pheromone is mostly evaporated and all ants lay new pheromone;

For Tour=2 to N_{tour}

{

All ants select paths based on pheromone;

Calculate paths' quality;

Find the best solution of the tour;

Update the best solution of all tours;

Existing pheromone is partially evaporated and all ants lay new pheromone;

}